DOI: 10.1478/AAPP.97S1A6

AAPP | Atti della Accademia Peloritana dei Pericolanti
*Classe di Scienze Fisiche, Matematiche e Naturali*
ISSN 1825-1242

Vol. 97, No. S1, A6 (2019)

# HIGH-FIELD MOBILITY IN GRAPHENE ON SUBSTRATE WITH A PROPER INCLUSION OF THE PAULI EXCLUSION PRINCIPLE

MARCO COCO [a], ARMANDO MAJORANA [a], GIOVANNI NASTASI [a] AND VITTORIO ROMANO [a*]

ABSTRACT. The aim of this work is to simulate charge transport in a monolayer graphene on different substrates. This requires the inclusion of the scatterings of charge carriers with impurities and phonons of the substrate, besides the interaction mechanisms already present in the graphene layer. As mathematical model, the semiclassical Boltzmann equation is assumed and the results are based on Direct Simulation Monte Carlo (DSMC) method. A crucial point is the correct inclusion of the Pauli Exclusion Principle (PEP). Most simulations use the approach proposed by Jacoboni e Lugli which, however, allows an occupation number greater than one with an evident violation of PEP. Here the Monte Carlo scheme devised by Romano et al. (J. Comput. Phys. **302**, 267–284, 2015) is employed. It predicts occupation numbers consistent with PEP and therefore is physically more accurate. Two different substrates are investigated: $SiO_2$ and hexagonal boron nitride (h-BN). We adopt the model for charge-impurities scattering described by E. H. Hwang and S. Das Sarma (Phys. Rev. B **75**, 205418, 2007). In such a model a crucial parameter is the distance $d$ between the graphene layer and the impurities of the substrate. Usually $d$ is considered constant. Here we assume that $d$ is a random variable in order to take into account the roughness of the substrate and the randomness of the location of the impurities. Our results confirm that h-BN is one of the most promising substrate also for the high-field mobility on account of the reduced degradation of the velocity due to the remote impurities. This is in agreement with results shown by Hirai *et al.* (J. Appl. Phys. **116**, 083703, 2014) where only the low-field mobility has been investigated.

## 1. Introduction

Graphene is a gapless semiconductor made of a single layer of carbon atoms arranged into a honeycomb lattice. The energy band structure of graphene has, as a first approximation, a conical band structure around the Dirac points. So electrons have a zero effective mass and they exhibit a photon-like behavior. A physically accurate model for charge transport is given by a semiclassical Boltzmann equation, whose scattering terms have been deeply analyzed in the last decade. Quantum effects have also been included in the literature but, for Fermi energies high enough, as those which are considered in this paper, the interband tunneling effect is practically negligible and the semiclassical approach reveals satisfactory (Kané *et al.* 2015). The aim of this work is to simulate a monolayer graphene on a substrate,

as, for instance, considered by Hirai *et al.* (2014) (see Fig. 1), at variance with the case of suspended graphene studied by (Romano *et al.* 2015). Usually the available solutions are

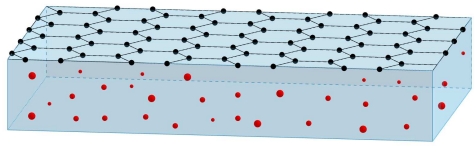

FIGURE 1. The graphene sheet over a substrate. The spheres represent the impurities.

obtained by means of DSMC. The peculiar band structure of graphene requires that the Pauli exclusion principle must be taken into account, but standard DSMC methods suffer from a violation of this principle, because they predict a maximum occupation number greater than one. Romano *et al.* (2015) have devised a new DSMC procedure in order to overcome such a difficulty and applied to charge transport in suspended monolayer graphene successfully. Comparisons with direct solutions of the electron Boltzmann equation, obtained by using a Discontinuous Galerkin (DG) method (Cockburn and Shu 1998), have confirmed the validity of the procedure (Coco *et al.* 2017).

Apart from the scatterings, already present in the suspended case, now we also need to include the effects of remote phonons and impurities of the substrate. The scattering rates between the electrons and the phonons of the substrate do not differ from the suspended case. The interactions with the impurities add noticeable additional difficulties, mainly due to the rather involved expression of the dielectric function, which is itself a source of theoretical debates (Hwang *et al.* 2007; Hwang and Das Sarma 2007).

We assume the model proposed by Hwang and Das Sarma (2007) for the charge-impurity scattering. A crucial parameter is the depth $d$ of the remote impurities. It is of the order of a few angstroms, but the exact value can vary from a specimen to another. $d$ has been considered constant by Coco *et al.* (2017) and the results for several values of $d$ have been shown.

Here we take into account the randomness of the impurity location, related also to the roughness of the interface of the oxide, by considering $d$ as a random variable. Some probability distributions have been analyzed: the uniform and the gamma with several choice of the parameters.

Two different substrates have been considered: $SiO_2$ and hexagonal boron nitride (h-BN). By Hirai *et al.* (2014) $HfO_2$ has been also considered, but the analysis at low fields reveals that it is not an adequate material because of the strong degradation of the mobilities. Our analysis confirms that h-BN is a better material than $SiO_2$, on account of the reduced degradation of the mobility and the stability with respect to the fluctuations of the parameter $d$, even if meaningful quantitative differences are found with respect to Hirai *et al.* (2014). h-BN assures the highest mobility, which does not suffer of randomness of the parameter $d$.

The plan of the paper is as follows. In Section 2, the semiclassical kinetic model for charge transport in graphene on a substrate is outlined. In Section 3, the adopted DSMC procedure is described in details and numerical results are presented.

## 2. Semiclassical charge transport in graphene on a substrate

In a semiclassical kinetic setting, the charge transport in graphene is described by four Boltzmann equations, one for electrons in the valence ($\pi$) band and one for electrons in the conduction ($\pi^*$) band, that in turn can belong to the $K$ or $K'$ valley,

$$\frac{\partial f_{\ell,s}(\mathrm{t},\mathbf{x},\mathbf{k})}{\partial \mathrm{t}} + \mathbf{v}_{\ell,s}\cdot\nabla_{\mathbf{x}} f_{\ell,s}(\mathrm{t},\mathbf{x},\mathbf{k}) - \frac{e}{\hbar}\mathbf{E}\cdot\nabla_{\mathbf{k}} f_{\ell,s}(\mathrm{t},\mathbf{x},\mathbf{k}) = \left(\frac{df_{\ell,s}}{d\mathrm{t}}(\mathrm{t},\mathbf{x},\mathbf{k})\right)_{coll}, \quad (1)$$

where $f_{\ell,s}(\mathrm{t},\mathbf{x},\mathbf{k})$ represents the distribution function of charge carriers in the valley $\ell$ ($K$ or $K'$), band $\pi$ or $\pi^*$ ($s=-1$ or $s=1$) at position $\mathbf{x}$, time t and wave-vector $\mathbf{k}$. We denote by $\nabla_{\mathbf{x}}$ and $\nabla_{\mathbf{k}}$ the gradients with respect to the position and wave-vector, respectively. The microscopic velocity $\mathbf{v}_{\ell,s}$ is related to the energy band $\varepsilon_{\ell,s}$ by

$$\mathbf{v}_{\ell,s} = \frac{1}{\hbar}\nabla_{\mathbf{k}}\,\varepsilon_{\ell,s}\,.$$

With a very good approximation (Castro Neto *et al.* 2009), a linear dispersion relation holds for the energy bands $\varepsilon_{\ell,s}$ around the equivalent Dirac points; so that $\varepsilon_{\ell,s} = s\hbar v_F\,|\mathbf{k}-\mathbf{k}_\ell|$, where $v_F$ is the (constant) Fermi velocity, $\hbar$ is the Planck constant divided by $2\pi$, and $\mathbf{k}_\ell$ is the position of the Dirac point $\ell$ in the first Brillouin zone. The elementary (positive) charge is denoted by $e$, and $\mathbf{E}$ is the electric field, here assumed to be constant. The right hand side of Eq. (1) is the collision term representing the interaction of electrons with impurities and phonons, the latter due to both the graphene crystal and substrate (Fang *et al.* 2011). Acoustic phonon scattering is intra-valley and intra-band. Optical phonon scattering is intra-valley and can be longitudinal optical ($LO$) and transversal optical ($TO$); moreover, it can be intra-band or inter-band. Scattering with optical phonons of type $K$ pushes electrons from a valley to the other one (inter-valley scattering). In addition to the interactions already present in the suspended case, surface optical phonon scattering and charged impurity (imp) scattering induced by the substrate are also included.

We assume that phonons are at thermal equilibrium. The general form of the collision operator can be written as

$$\begin{aligned}\left(\frac{df_{\ell,s}}{d\mathrm{t}}(\mathrm{t},\mathbf{x},\mathbf{k})\right)_{coll} \;=\; \sum_{\ell',s'}\Bigg[&\int_{\mathbb{R}^2} S_{\ell',s',\ell,s}(\mathbf{k}',\mathbf{k})\, f_{\ell',s'}(\mathrm{t},\mathbf{x},\mathbf{k}')\left(1-f_{\ell,s}(\mathrm{t},\mathbf{x},\mathbf{k})\right)d\mathbf{k}' \\ &- \int_{\mathbb{R}^2} S_{\ell,s,\ell',s'}(\mathbf{k},\mathbf{k}')\, f_{\ell,s}(\mathrm{t},\mathbf{x},\mathbf{k})\left(1-f_{\ell',s'}(\mathrm{t},\mathbf{x},\mathbf{k}')\right)d\mathbf{k}'\Bigg]\end{aligned}$$

where the scattering rate $S_{\ell',s',\ell,s}(\mathbf{k}',\mathbf{k})$ is given by the sum of terms of kind

$$\begin{aligned}\left|G^{(\nu)}_{\ell',s',\ell,s}(\mathbf{k}',\mathbf{k})\right|^2 \Big[&\left(n^{(\nu)}_{\mathbf{q}}+1\right)\delta\left(\varepsilon_{\ell,s}(\mathbf{k})-\varepsilon_{\ell',s'}(\mathbf{k}')+\hbar\,\omega^{(\nu)}_{\mathbf{q}}\right) \\ &+ n^{(\nu)}_{\mathbf{q}}\,\delta\left(\varepsilon_{\ell,s}(\mathbf{k})-\varepsilon_{\ell',s'}(\mathbf{k}')-\hbar\,\omega^{(\nu)}_{\mathbf{q}}\right)\Big] \qquad (2)\end{aligned}$$

related to electron-phonon scatterings and other terms corresponding to the scatterings with the impurities.

The index $\nu$ labels the $\nu$th phonon mode and $G^{(\nu)}_{\ell',s',\ell,s}(\mathbf{k}',\mathbf{k})$ is the kernel, which describes the scattering mechanism, due to phonons $\nu$, between electrons belonging to valley $\ell'$ and band $s'$, and electrons belonging to valley $\ell$ and band $s$. The symbol $\delta$ denotes the Dirac

distribution, $\omega_{\mathbf{q}}^{(\nu)}$ is the $\nu$th phonon frequency, $n_{\mathbf{q}}^{(\nu)}$ is the Bose-Einstein distribution for the phonon of type $\nu$

$$n_{\mathbf{q}}^{(\nu)} = \frac{1}{e^{\hbar\,\omega_{\mathbf{q}}^{(\nu)}/k_B T} - 1},$$

$k_B$ is the Boltzmann constant and $T$ the constant graphene lattice temperature. The scattering with a phonon $\nu_*$ can be assumed elastic if $\hbar\,\omega_{\mathbf{q}}^{(\nu_*)} \ll k_B T$. In this case, in Eq. (2) we eliminate the term $\hbar\,\omega_{\mathbf{q}}^{(\nu_*)}$ inside the delta distribution and we use the approximation $n_{\mathbf{q}}^{(\nu_*)} \approx k_B T/\hbar\,\omega_{\mathbf{q}}^{(\nu)} - \frac{1}{2}$.

We will describe the terms of the collision operator concerning the scatterings with the impurities in the sequel.

**2.1. The model with only one distribution function.** By applying a gate voltage or a transversal electric field with respect to the graphene sheet, it is possible to modify the Fermi energy $\varepsilon_F$ and therefore the charge density. If a high positive value of the Fermi energy is considered, the electrons responsible for the current are those belonging to the conduction band. Therefore, only the transport equation for electrons in the conduction band is considered and inter-band electron transitions are neglected. Moreover, the valleys $K$ and $K'$ are considered as equivalent. A reference frame centered in the $K$-point will be used. We simplify the notation, omitting the indexes $s$ and $\ell$ and denoting by $f$ the only relevant distribution function.

The expressions of the electron-phonon scattering matrices used in our simulations are as follows.

For acoustic phonons, usually one considers the elastic approximation, and therefore

$$\left(2\,n_{\mathbf{q}}^{(ac)} + 1\right)\left|G^{(ac)}(\mathbf{k}',\mathbf{k})\right|^2 = \frac{1}{(2\,\pi)^2}\,\frac{\pi\,D_{ac}^2\,k_B\,T}{2\hbar\,\sigma_m\,v_p^2}\left(1+\cos\vartheta_{\mathbf{k},\mathbf{k}'}\right), \tag{3}$$

where $D_{ac}$ is the acoustic phonon coupling constant, $v_p$ is the sound speed in graphene, $\sigma_m$ the graphene areal density, and $\vartheta_{\mathbf{k},\mathbf{k}'}$ is the convex angle between $\mathbf{k}$ and $\mathbf{k}'$.

There are three relevant optical phonon scatterings: the longitudinal optical ($LO$), the transversal optical ($TO$) and the $K$ phonons. The electron-phonon scattering matrices are

$$\left|G^{(LO)}(\mathbf{k}',\mathbf{k})\right|^2 = \frac{1}{(2\,\pi)^2}\,\frac{\pi\,D_O^2}{\sigma_m\,\omega_O}\left(1-\cos(\vartheta_{\mathbf{k},\mathbf{k}'-\mathbf{k}}+\vartheta_{\mathbf{k}',\mathbf{k}'-\mathbf{k}})\right), \tag{4}$$

$$\left|G^{(TO)}(\mathbf{k}',\mathbf{k})\right|^2 = \frac{1}{(2\,\pi)^2}\,\frac{\pi\,D_O^2}{\sigma_m\,\omega_O}\left(1+\cos(\vartheta_{\mathbf{k},\mathbf{k}'-\mathbf{k}}+\vartheta_{\mathbf{k}',\mathbf{k}'-\mathbf{k}})\right), \tag{5}$$

$$\left|G^{(K)}(\mathbf{k}',\mathbf{k})\right|^2 = \frac{1}{(2\,\pi)^2}\,\frac{2\pi\,D_K^2}{\sigma_m\,\omega_K}\left(1-\cos\vartheta_{\mathbf{k},\mathbf{k}'}\right), \tag{6}$$

where $D_O$ is the optical phonon coupling constant, $\omega_O$ is the optical phonon frequency, $D_K$ is the K-phonon coupling constant and $\omega_K$ is the $K$-phonon frequency. The angles $\vartheta_{\mathbf{k},\mathbf{k}'-\mathbf{k}}$ and $\vartheta_{\mathbf{k}',\mathbf{k}'-\mathbf{k}}$ denote the convex angles between $\mathbf{k}$ and $\mathbf{k}'-\mathbf{k}$ and between $\mathbf{k}'$ and $\mathbf{k}'-\mathbf{k}$, respectively.

Due to the presence of the substrate, we have to include also the interactions between the electrons of the graphene sheet and the remote phonons and impurities of the substrate. The corresponding electron-phonon scattering matrices have the same form of (4) and (5) but

different physical parameters. Regarding the remote impurity scatterings, we assume that the remote impurities stay in a plane at distance $d$ from the graphene sheet. The definition of the scattering rate for electron-impurity scattering is highly complex; so many approximate models are proposed. Following Hwang and Das Sarma (2007), we adopt the expression

$$S^{(imp)}(\mathbf{k},\mathbf{k}') = \frac{2\pi}{\hbar}\,\frac{n_i}{(2\pi)^2}\left|\frac{V_i(|\mathbf{k}-\mathbf{k}'|,d)}{\varepsilon(|\mathbf{k}-\mathbf{k}'|)}\right|^2 \frac{\left(1+\cos\vartheta_{\mathbf{k},\mathbf{k}'}\right)}{2}\,\delta\left(\varepsilon(\mathbf{k}')-\varepsilon(\mathbf{k})\right), \qquad (7)$$

where

a) $n_i$ is the number of impurities per unit area.

b) $V_i(|\mathbf{k}-\mathbf{k}'|,d) = 2\pi e^2\,\dfrac{\exp(-d\,|\mathbf{k}-\mathbf{k}'|)}{\tilde{\kappa}\,|\mathbf{k}-\mathbf{k}'|}$

- $d$ is the location of the charged impurity measured from the graphene sheet
- $\tilde{\kappa}$ is the effective dielectric constant, defined by $4\pi\varepsilon_0\left(\kappa_{top}+\kappa_{bottom}\right)/2$, where $\varepsilon_0$ is the vacuum dielectric constant and $\kappa_{top}$ and $\kappa_{bottom}$ are the relative dielectric constants of the medium above and below the graphene layer. For example, if the materials are $SiO_2$ and air one has $\tilde{\kappa} = 4\pi\varepsilon_0\left(1+\kappa_{SiO_2}\right)/2 \approx 4\pi\times 2.45\,\varepsilon_0$.

c) $\varepsilon(|\mathbf{k}-\mathbf{k}'|) = \begin{cases} 1+\dfrac{q_s}{|\mathbf{k}-\mathbf{k}'|}-\dfrac{\pi q_s}{8k_F} & \text{if } |\mathbf{k}-\mathbf{k}'|<2k_F \\ 1+\dfrac{q_s}{|\mathbf{k}-\mathbf{k}'|}-\dfrac{q_s\sqrt{|\mathbf{k}-\mathbf{k}'|^2-4k_F^2}}{2|\mathbf{k}-\mathbf{k}'|^2}-\dfrac{q_s}{4k_F}\operatorname{asin}\left(\dfrac{2k_F}{|\mathbf{k}-\mathbf{k}'|}\right) & \text{otherwise} \end{cases}$

is the 2D finite temperature static random phase approximation (RPA) dielectric (screening) function appropriate for graphene;

- $q_s = \dfrac{4e^2k_F}{\tilde{\kappa}\hbar v_F}$ is the effective Thomas-Fermi wave-vector for graphene; it can be rewritten in terms of the dimensionless Wigner-Seitz radius $r_S$ as $q_s = 4r_S k_F$;
- $k_F = \dfrac{\varepsilon_F}{\hbar v_F}$ is the Fermi wave-vector.

The parameter $d$ is usually fixed once for all in each simulation. However it is more realistic to assume that $d$ can vary because the impurities are implanted with a certain degree of uncertainty in their location. As already shown by Coco *et al.* (2017), $d$ is crucial for a correct prediction of the electron velocity, and therefore, in turn, of the electron mobilities. In the present paper we assume that $d$ is a random variable. A uniform distribution and gamma distributions with several values of the parameters will be considered. The choice of the latter ones is due to their flexibility to model the distance of the impurities.

We close this section evaluating the transition rates (collision frequencies) associated to the scattering mechanisms introduced above. For the $A$th type of scattering the transition rate is defined as

$$\Gamma_A(\mathbf{k}) = \int_{\mathbb{R}^2} S_A(\mathbf{k},\mathbf{k}')\,d\mathbf{k}'$$

and depends on $\mathbf{k}$ only through the energy, that is indeed $\Gamma_A(\mathbf{k}) = \Gamma_A(\varepsilon)$.

For the acoustic phonon scattering we get

$$\Gamma_{ac}(\varepsilon) = \frac{D_{ac}^2 k_B T}{4\hbar^3 v_F^2 \sigma_m v_p^2} \varepsilon \tag{8}$$

while for the total optical phonon scattering, given by the sum of the longitudinal and transversal contribution, we have

$$\Gamma_{op}(\varepsilon) = \frac{D_O^2}{\sigma_m \omega_O \hbar^2 v_F^2} \left[ (\varepsilon - \hbar\omega_O) \left( n_{\mathbf{q}}^{(O)} + 1 \right) H(\varepsilon + \hbar\omega_O) + (\varepsilon + \hbar\omega_O) n_{\mathbf{q}}^{(O)} \right], \tag{9}$$

where the fact that the coupling constants are the same for both the longitudinal and the transversal optical phonons has been used. In Eq. (9) $H$ is the Heaviside function and $n_{\mathbf{q}}^{(O)}$ the equilibrium optical phonon distribution.

The expression of the transition rate for the $K$ phonon scattering is the same as for the optical phonon

$$\Gamma_K(\varepsilon) = \frac{D_K^2}{\sigma_m \omega_K \hbar^2 v_F^2} \left[ (\varepsilon - \hbar\omega_K) \left( n_{\mathbf{q}}^{(K)} + 1 \right) H(\varepsilon - \hbar\omega_K) + (\varepsilon + \hbar\omega_K) n_{\mathbf{q}}^{(K)} \right]. \tag{10}$$

Above $n_{\mathbf{q}}^{(K)}$ is the equilibrium $K$ phonon distribution. At last the transition rate for the impurity scattering, due to the rather involved expression, has to be evaluated numerically. According to a well-known procedure, the following correction is adopted (Lundstrom 2000)

$$\Gamma_{imp}(\mathbf{k}) = \int_{\mathbb{R}^2} S^{(imp)}(\mathbf{k}, \mathbf{k}') \left( 1 - \cos\vartheta_{\mathbf{k},\mathbf{k}'} \right) d\mathbf{k}'. \tag{11}$$

The physical parameters for the scattering rates are summarized in Tabs. 1-2 and are the same as by Hirai *et al.* (2014).

TABLE 1. Physical parameters for the scattering rates in pristine graphene.

| | | | |
|---|---|---|---|
| $v_F$ | $10^8$ cm/s | $v_p$ | $2 \times 10^6$ cm/s |
| $\sigma_m$ | $7.6 \times 10^{-8}$ g/cm$^2$ | $D_{ac}$ | 6.8 eV |
| $\hbar\omega_O$ | 164.6 meV | $D_O$ | $10^9$ eV/cm |
| $\hbar\omega_K$ | 124 meV | $D_K$ | $3.5 \times 10^8$ eV/cm |

TABLE 2. Physical parameters for the scattering rates related to the substrates.

| | $SiO_2$ | h-BN |
|---|---|---|
| $\hbar\omega_{op-ac}$ | 55 meV | 200 meV |
| $D_f$ | $5.14 \times 10^7$ eV/cm | $1.29 \times 10^9$ eV/cm |
| $n_i$ | $2.5 \times 10^{11}$ cm$^{-2}$ | $2.5 \times 10^{10}$ cm$^{-2}$ |
| $\kappa_{bottom}$ | 3.9 | 3 |

We look for spatially homogeneous solutions to Eq. (1) under a constant applied electric field. In such a case the transport equation reduces to

$$\frac{\partial f(\mathrm{t},\mathbf{k})}{\partial \mathrm{t}} - \frac{e}{\hbar}\,\mathbf{E}\cdot\nabla_{\mathbf{k}} f(\mathrm{t},\mathbf{k}) = \int_{\mathbb{R}^2} S(\mathbf{k}',\mathbf{k})\, f(\mathrm{t},\mathbf{k}')\,(1-f(\mathrm{t},\mathbf{k}))\,d\mathbf{k}' - \int_{\mathbb{R}^2} S(\mathbf{k},\mathbf{k}')\, f(\mathrm{t},\mathbf{k})\,\big(1-f(\mathrm{t},\mathbf{k}')\big)\,d\mathbf{k}'. \tag{12}$$

We take a Fermi-Dirac distribution as initial condition, *i.e.*

$$f(0,\mathbf{k}) = \frac{1}{1+\exp\left(\dfrac{\varepsilon(\mathbf{k})-\varepsilon_F}{k_B T}\right)},$$

where $T = 300\,\mathrm{K}$ is the room lattice temperature which will be assumed constant.

## 3. DSMC method

We have also used, for solving the transport equation (1), the ensemble DSMC method recently proposed by Romano *et al.* (2015). The $\mathbf{k}$-space is approximated by the set $[-k_{xmax}, k_{xmax}] \times [-k_{ymax}, k_{ymax}]$ with $k_{xmax}$ and $k_{ymax}$ such that the number of electrons with a wave-vector $\mathbf{k}$ outside such a set is practically negligible. The $\mathbf{k}$-space is partitioned into a uniform rectangular grid. We shall denote by $C_{ij}$ the generic cell of the grid centered at the $\mathbf{k}_{ij}$ wave-vector.

The distribution function is approximated with a piecewise constant function in each cell. At time $t = 0$ the $n_P$ particles used for the simulation are distributed in each cell according to the equilibrium Fermi-Dirac distribution.

The motion of each particle alternates free-flight and scattering. The latter is the most involved and delicate part and it is particularly important to include PEP to describe charge transport in graphene correctly. This implies a heavy computational cost and requires an update of the distribution function at each time step.

Now we describe the numerical scheme for the electron-phonon collision. The time interval $\Delta\mathrm{t}$ is chosen for each particle in a random way by means of

$$\Delta\mathrm{t} = -\frac{\ln\xi}{\Gamma_{tot}(\varepsilon(\mathrm{t}))}, \tag{13}$$

where $\xi$ is a random number with uniform distribution in the interval $[0,1]$ and $\Gamma_{tot}$ being the total scattering rate of the particle, having energy $\varepsilon$ at time t.

$$\Gamma_{tot}(\varepsilon(\mathrm{t})) = \Gamma_{ac}(\varepsilon(\mathrm{t})) + \Gamma_{op}(\varepsilon(\mathrm{t})) + \Gamma_K(\varepsilon(\mathrm{t})) + \Gamma_{imp}(\varepsilon(\mathrm{t})) + \Gamma_{ss}(\varepsilon(\mathrm{t})).$$

The function $\Gamma_{ss}$, called *self-scattering rate*, is the scattering rate associated to a fictitious scattering that does not change the state of the electron. The self-scattering rate is determined by considering the sum $\Gamma_M = \Gamma_{ac} + \Gamma_{op} + \Gamma_K + \Gamma_{imp}$. Hence $\Gamma_{ss}$ is fixed in such a way $\Gamma_{tot} = \alpha\Gamma_M$, where $\alpha > 1$ is a tuning parameter. We set $\alpha = 1.1$ in our simulations. This method differs from the standard one (Jacoboni and Lugli 1989).

The scattering is selected randomly according to the values of the transition rates, and PEP is taken into account as by Lugli and Ferry (1985). Once the state after the scattering has been determined, denoted by $\mathbf{k}'$ its wave-vector, the initial state is changed or left the same according to the rejection technique. It consists to choose a random number $\xi$

generated uniformly in $[0,1]$ and, if $\xi < 1 - f(\mathbf{k}')$ the transition is accepted, otherwise it is rejected. Then, according to the angular distribution of the scattering rate, a rejection method allows to select the angular dependence of the wave-vector after the scattering event.

At fixed times the momentum, velocity, energy of each electron are stored and the mean values are evaluated in order to follow the time evolution of the system.

The maximum number $n_{ij}^*$ of simulated particles accommodated in each cell is easily evaluated (Lugli and Ferry 1985). Let $N_{ij}$ be the number of real particles in the cell $C_{ij}$ and let $n_{ij}$ be the number of simulated particles in the same cell. Let $A$ be the area of the sample and let $N$ be the number of real particles in the sample, $N = \rho A$. By observing that $N/n_P$ is the statistical weight of each particle entering the simulation and taking into account the condition $0 \leq f \leq 1$, one has

$$\begin{aligned} n_{ij} &= \frac{N_{ij}}{N} n_P = \frac{n_P}{N} \frac{2}{(2\pi)^2} A \int_{C_{ij}} f \, d\mathbf{k} \leq \frac{n_P}{N} \frac{2}{(2\pi)^2} A \int_{C_{ij}} d\mathbf{k} \\ &= \frac{2}{(2\pi)^2} \mathrm{meas}(C_{ij}) \frac{n_P}{N} A = \frac{2}{(2\pi)^2} \mathrm{meas}(C_{ij}) \frac{n_P}{\rho} = n_{ij}^*, \end{aligned} \tag{14}$$

where $\mathrm{meas}(C_{ij})$ is the measure of the cell $C_{ij}$. Of course $n_{ij}^*$ is not in general an integer, therefore rounding errors are introduced. Usually the problem is solved by using a number of simulated particles $n_P$ great enough to make such errors negligible. The convergence of the procedure is often checked just by comparing the results with different $n_P$.

In the standard approach the free-flight is performed according to the semiclassical equation of motion

$$\hbar \dot{\mathbf{k}} = -e \, \mathbf{E}. \tag{15}$$

The main concern with the procedure delineated above is that, according to the semiclassical approximation, the compatibility with Pauli's exclusion principle during the free flight is not checked. *It may occur that the particle at the end of the free-flight reaches a cell in the* $\mathbf{k}$*-space already fully occupied making the occupation number greater than one* (Romano *et al.* 2015).

It is of course unphysical the fact that, for high values of the Fermi energy, the maximum occupation number can greatly exceed the maximum one, although the average quantities could be acceptable according to the law of large numbers. Even if the scattering can redistribute the particles among the cells, in general it is not possible to eliminate the presence of anomalous occupation numbers.

For overcoming the problem, Tadyszak *et al.* (1998) have proposed to apply the rejection technique not only to the scattering events but also at the end of each free-flight. However, even implementing this variant, the same drawbacks are still present as shown by Romano *et al.* (2015).

In order to avoid such a difficulty, Romano *et al.* (2015) have proposed the following approach. The crucial point in the previous procedure is the step concerning the free-flight. If we go back to the original transport equation, we can use a splitting scheme to avoid unphysical results. The basic idea is to reformulate the splitting method in terms of a particle method.

In a time interval $\Delta t$, first we solve the drift part of the equation corresponding to the free-flight in the analogous DSMC approach,

$$\frac{\partial f(t,\mathbf{x},\mathbf{k})}{\partial t} - \frac{e}{\hbar}\mathbf{E}\cdot\nabla_{\mathbf{k}} f(t,\mathbf{x},\mathbf{k}) = 0, \tag{16}$$

taking as initial condition the distribution at time t, and then the collision part

$$\frac{\partial f(t,\mathbf{x},\mathbf{k})}{\partial t} = \left(\frac{df}{dt}(t,\mathbf{x},\mathbf{k})\right)_{coll}, \tag{17}$$

taking as initial condition the solution of Eq. (16). The global procedure gives a numerical approximation of $f(t+\Delta t,\mathbf{x},\mathbf{k})$ up to first order in $\Delta t$. The solution of Eq. (16) is just a *rigid* translation of the distribution function along the characteristics and can be reformulated from a particle point of view as a free-flight of the same time step for each electron. In this way, the cells in the $\mathbf{k}$-space are moved of the displacement vector $\hbar\Delta\mathbf{k} = -e\mathbf{E}\Delta t$ but without changing the occupation number of the cells themselves. To avoid considering a computational domain too large, we adopt a Lagrangian approach and move the grid by adapting it to the new position of the cells, instead of moving the cells themselves.

Eq. (17) is solved by a sequence of collision steps for each particle during the time interval $[t, t+\Delta t]$ in a standard way. Since the collision mechanisms take into account PEP, the occupation number cannot exceed the maximum occupation number in this second step as well. Hence, neither the drift nor the collision step give rise to the possibility of having, in a single cell, more particles than the maximum occupation number.

The overall scheme is a hybrid approach which furnishes a first order in time approximation of the distribution function. Average quantities can be evaluated as well by taking the mean values of the quantities of interest, e.g. velocity and energy.

## 4. Numerical results

The simulations are performed at several values of the electric field and Fermi energy.

In order to validate the simulation approach, we numerically solve, in the case of constant $d$, the Boltzmann equation by using a DG method (see (Coco *et al.* 2017) for the details), obtaining an excellent agreement.

The parameter $d$ should be of the order of few angstroms. In the literature a range from 0 to 1 nm is considered. At variance with Coco *et al.* (2017), $d$ is considered a random variable. Therefore, in the simulation whenever a scattering with impurities occurs, $d$ is generated according to the chosen distribution. We compare DSMC results, considering $d$ both constant and random, with the numerical solutions of the Boltzmann equation obtained by using DG method with a constant $d$ only.

Conservation of the number of electrons implies that the charge density $\rho$, given by

$$\rho = \frac{2}{(2\pi)^2}\int_{\mathbb{R}^2} f(t,\mathbf{k})\, d\mathbf{k}, \tag{18}$$

is constant in time.

We choose a reference frame such that only the $x-$component of the electric field is different from 0; therefore only the $x-$component of the mean velocity is relevant. $10^5$ particles have been used in the DSMC method.

In Figs. 2-4, we show the numerical results of the average velocity $\mathbf{v}$ defined as

$$\mathbf{v}(\mathrm{t}) = \frac{2}{(2\pi)^2 \rho} \int_{\mathbb{R}^2} f(\mathrm{t},\mathbf{k}) \frac{1}{\hbar} \nabla_{\mathbf{k}} \varepsilon(\mathbf{k})\, d\mathbf{k}, \tag{19}$$

and is related to the mobility $\mu(\mathbf{E})$ as follows

$$\mathbf{v} = \mu(\mathbf{E})\mathbf{E}.$$

The current $\mathbf{J}$ is given by

$$\mathbf{J} = -e\rho\mathbf{v}.$$

From the analysis of the average velocity, it is possible to estimate the effect of the impurities on the mobility. It is expected that the scattering with the remote impurities leads to a degradation of the mobility depending on the specific material.

First, we have assessed the general performance of the different materials by a comparison of the average velocity for three different constant values of $d$.

We observe that the values of the average velocity and energy become lower by reducing the distance $d$ from the impurities in the oxide, confirming the degradation of the mobility due to the substrate as a direct consequence of the additional scatterings with the remote impurities. For the highest value of $d$, which is very close to the pristine case, both $SiO_2$ and h-BN produce of course the same effect, with a comparable electron velocity. For the intermediate value of $d$, h-BN performs better than $SiO_2$ and this behavior is even more evident for $d = 1$ nm. Therefore, h-BN gives a better high-field mobility, in qualitative agreement with the low field analysis by Hirai *et al.* (2014).

The previous results, however, do not take into account the intrinsic noise in the location of the impurities. In order to assess its effect on the high-field mobility, we have performed some simulations with a random $d$ generated, in each scattering involving impurities, according to a prescribed probability distribution (see Fig. 4). First we have considered a uniform distribution in the interval $[0,1]$ (in nm). The results are similar to those of the case with constant $d = 0.5$ nm and this can be explained by observing that 0.5 is the expectation value. Afterwards, we have considered a $\Gamma(\alpha,\lambda)$ distribution

$$f(x) = \begin{cases} \dfrac{1}{\lambda\Gamma(\alpha)} x^{\alpha-1} e^{x/\lambda} & x > 0 \\ 0 & x \leq 0 \end{cases}$$

where $\Gamma(\alpha)$ is the Euler gamma function. We have used the values $\lambda = 0.5$ and $\alpha = 2,3,4$ (see Fig. 5) and rescaled $d$ by a factor 0.2 in order to have values less than 1 with very high probability, as confirmed by the simulation.

In order to validate our findings, the results obtained by using the DG method by Coco *et al.* (2017) but with a value of $d$ set equal to the mean values of the considered distribution (the mean value of $\Gamma(\alpha,\lambda)$ is $\alpha\lambda$) rescaled by the factor 0.2. The agreement is still excellent.

We would like to remark that both the materials seem only slightly influenced by the stochastic effect related to the randomness of the impurity positions.

## 5. Conclusions

An analysis of the high-field mobility has been performed for graphene on a substrate by a new DSMC approach, which properly takes into account the Pauli exclusion principle.

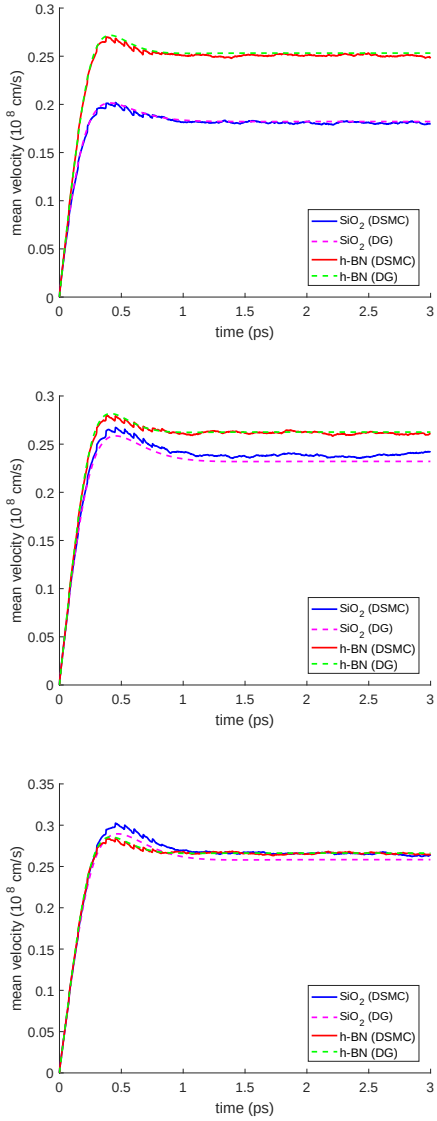


FIGURE 2. Comparison of the average velocity versus time for $d = 0$ (top) , 0.5, 1 (bottom) nm in the case of an applied electric field of 5 kV/cm and Fermi energy $\varepsilon_F = 0.4$ eV. Both the results obtained by using the DSMC and the DG method are reported.

The same substrates as by Hirai *et al.* (2014) have been considered but including the more accurate model for the charge-impurities scattering, proposed by Hwang and Das Sarma (2007). Moreover, also the random distribution of the depth of the impurities implanted

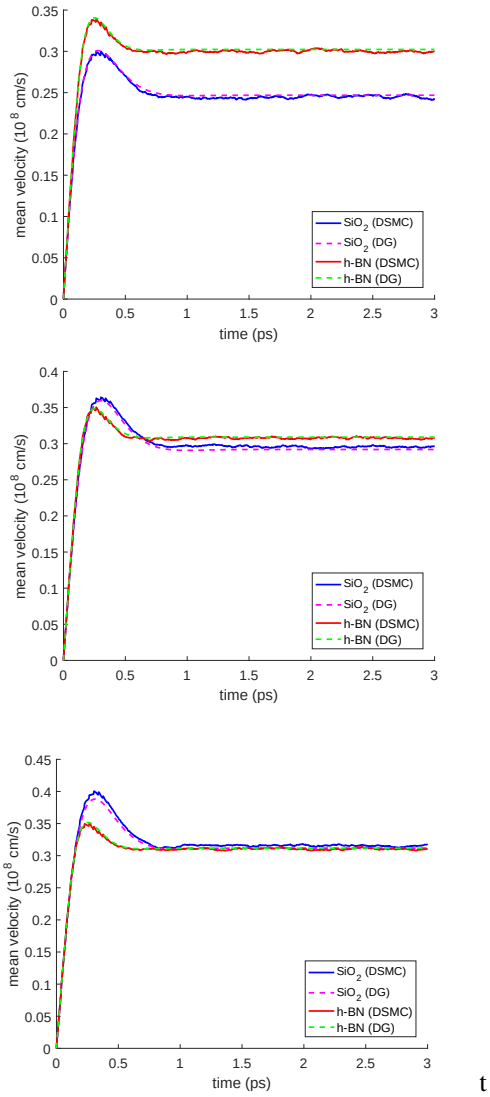


FIGURE 3. Comparison of the average velocity versus time for $d = 0$ (top) , 0.5, 1 (bottom) nm in the case of an applied electric field of 10 kV/cm and Fermi energy $\varepsilon_F = 0.4$ eV. Both the results obtained by using the DSMC and the DG method are reported.

in the oxide has been taken into account and described with several theoretical probability distributions. The differences among the average velocities for the considered substrates are in agreement with the expected effects and confirm a degradation of the mobility. As already

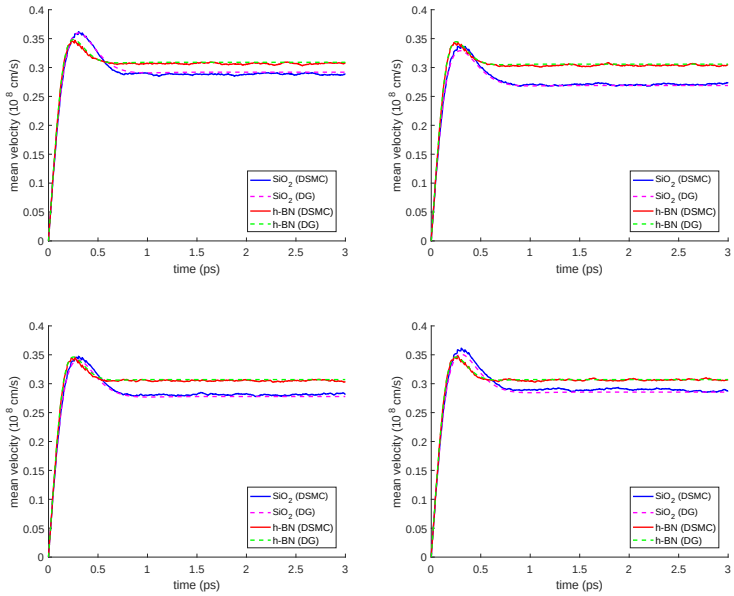


FIGURE 4. Comparison of the average velocity versus time in the case of an applied electric field of 10 kV/cm and Fermi energy $\varepsilon_F = 0.4$ eV by considering different distributions for $d$: uniform (top left), $\Gamma(2,0.5)$ (top right), $\Gamma(3,0.5)$ (bottom left), $\Gamma(4,0.5)$ (bottom right). In the results obtained with the DG method we have assumed $d$ equal to the mean value of the corresponding distribution rescaled by the factor 0.2.

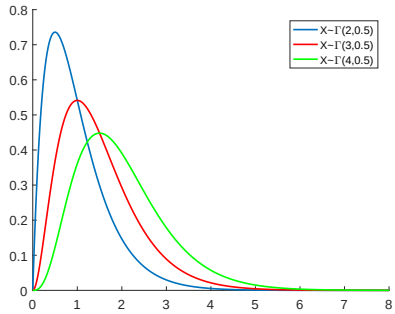


FIGURE 5. Plot of the $\Gamma(\alpha,\lambda)$ distribution with $\lambda = 0.5$ and $\alpha = 2,3,4$. Note that the probability to generate a number greater than 5 is practically zero.

found out by Hirai *et al.* (2014) for the low field mobility, h-BN reveals a better substrate than $SiO_2$, because it produces a smaller degradation also in the high-field mobility.

## Acknowledgments

This work has been partially supported by the University of Catania, project F.I.R. *Charge transport in graphene and low dimensional systems*, and by INdAM.

## References

Castro Neto, A. H., Guinea, F., Peres, N. M. R., Novoselov, K. S., and Geim, A. K. (2009). "The electronic properties of graphene". *Reviews of Modern Physics* **81**, 109–162. DOI: 10.1103/RevModPhys.81.109.

Cockburn, B. and Shu, C.-W. (1998). "The local discontinuous Galerkin method for convection-diffusion systems". *SIAM Journal on Numerical Analysis* **35**(6), 2440–2463. DOI: 10.1137/S0036142997316712.

Coco, M., Majorana, A., and Romano, V. (2017). "Cross validation of discontinuous Galerkin method and Monte Carlo simulations of charge transport in graphene on substrate". *Ricerche di Matematica* **66**, 201–220. DOI: 10.1007/s11587-016-0298-4.

Fang, T., Konar, A., Xing, H., and Jena, D. (2011). "High-field transport in two-dimensional graphene". *Physical Review B* **84**, 125450. DOI: 10.1103/PhysRevB.84.125450.

Hirai, H., Tsuchiya, H., Kamakura, Y., Mori, N., and Ogawa, M. (2014). "Electron mobility calculation for graphene on substrates". *Journal of Applied Physics* **116**, 083703. DOI: 10.1063/1.4893650.

Hwang, E. H., Adam, S., and Das Sarma, S. (2007). "Carrier transport in two-dimensional graphene layers". *Physical Review Letters* **98**, 186806. DOI: 10.1103/PhysRevLett.98.186806.

Hwang, E. H. and Das Sarma, S. (2007). "Dielectric function, screening, and plasmon in two-dimensional graphene". *Physical Review B* **75**, 205418. DOI: 10.1103/PhysRevB.75.205418.

Jacoboni, C. and Lugli, P. (1989). *The Monte Carlo Method for Semiconductor Device Simulation*. Springer-Verlag Wien. DOI: 10.1007/978-3-7091-6963-6.

Kané, G., Lazzeri, M., and Mauri, F. (2015). "High-field transport in graphene: the impact of Zener tunneling". *Journal of Physics: Condensed Matter* **27**, 164205. DOI: 10.1088/0953-8984/27/16/164205.

Lugli, P. and Ferry, D. K. (1985). "Degeneracy in the ensemble Monte Carlo method for high-field transport in semiconductors". *IEEE Transactions on Electron Devices* **32**(11), 2431–2437. DOI: 10.1109/T-ED.1985.22291.

Lundstrom, M. (2000). *Fundamentals of Carrier Transport*. Cambridge University Press. DOI: 10.1017/CBO9780511618611.

Romano, V., Majorana, A., and Coco, M. (2015). "DSMC method consistent with Pauli exclusion principle and comparison with deterministic solutions for charge transport in graphene". *Journal of Computational Physics* **302**, 267–284. DOI: 10.1016/j.jcp.2015.08.047.

Tadyszak, P., Danneville, F., and Cappy, A. (1998). "Monte Carlo calculations of hot-carrier noise under degenerate conditions". *Applied Physics Letters* **69**(10), 1450–1452. DOI: 10.1063/1.117611.

[a] Università degli Studi di Catania
Dipartimento di Matematica e Informatica
Viale A. Doria 6, 95125 Catania, Italy

* To whom correspondence should be addressed | email: romano@dmi.unict.it

Paper contributed to the conference entitled "Thermal theories of continua: survey and developments (Thermocon 2016)", which was held in Messina, Italy (19–22 April 2016) under the patronage of the *Accademia Peloritana dei Pericolanti*
Manuscript received 31 October 2017; published online 20 May 2019